Possibilities of Coherent X-ray Production with ERL

I.V. Bazarov
Wilson Lab, Cornell University, Ithaca, NY 14853

Abstract
By finessing limitations of storage rings, ERLs are capable of producing very bright electron beams with high electron density in 6D phase space and average current of about 100 mA. ERL based light source employs undulators to generate hard X-rays. Undulator can be used in two modes: spontaneous synchrotron radiation (SR) and, if undulator is sufficiently long and electron beam quality is sufficiently high, amplified spontaneous emission regime. While the former does not put any special requirements on electron beam quality or undulators, the latter is significantly more efficient in producing coherent photons per electron. The properties of X-ray radiation from these two different approaches of X-ray production are reviewed and a possibility of using amplified spontaneous emission at ERL is looked into.

Undulator as an X-ray source

An experimenter who employs hard X-rays is interested in the light source that possesses several key parameters: wavelength λ (~ 1 Å), small bandwidth $\Delta\lambda/\lambda = \Delta\omega/\omega$ (from 10^{-2} to as low as 10^{-4}), small source size and divergence. All these parameters are interrelated in a planar undulator's radiation, which is used to produce X-rays of n^{th} harmonic with wavelength, λ_n, given by

$$\lambda_n = \frac{\lambda_p}{2\gamma^2 n}\left[1 + \tfrac{1}{2}K^2 + \gamma^2\theta^2\right]. \qquad (1)$$

The notations here have their usual meaning: λ_p is undulator period, γ is relativistic factor, θ is the angle of emission with respect to the electron beam axis, $K = 0.934B[T]\cdot\lambda_p[cm]$ is dimensionless strength parameter for peak undulator field of B, which, for a hybrid permanent magnet ($SmCo_5$) design with a ratio of gap to undulator period $\kappa = g/\lambda_p$ is given by [1]:

$$B[T] \approx 3.33\exp[-\kappa(5.47 - 1.8\kappa)]. \qquad (2)$$

Only the fundamental harmonic is present when $K << 1$, and higher harmonics appear for bigger K values due to the fact that longitudinal velocity of electron, $\beta_z = \dot{z}/c$, in the undulator oscillates around the average velocity $\overline{\beta}_z \cong 1 - 1/2\gamma^2 - K^2/4\gamma^2$ with an amplitude of $K^2/4\gamma^2$ at twice the "wiggle" frequency $\overline{\beta}_z c/\lambda_p$. In a helical undulator, such modulation of longitudinal velocity is absent, thus, there are no higher order harmonics in the spectrum [2]. Furthermore, only odd harmonics are present in the forward direction for a planar undulator, while even harmonics can be observed in a

nonforward direction [3].

In addition to (1), there is a bandwidth (FWHM) of n^{th} harmonic due to a finite number of undulator poles, N_{p}:

$$\frac{\Delta\lambda}{\lambda_n} \approx \frac{1}{nN_{\text{p}}}. \qquad (3)$$

Expression (3) determines the minimum photon bandwidth achievable without a monochromator for electron beam with no energy spread.

I. Spontaneous SR

Central cone

First, we consider undulator radiation from a cold electron beam (no emittance) of current *I*. Combining expressions (3) and (1), it can be seen that useful X-rays from an undulator are found in the central cone within an opening angle determined from $\gamma^2\theta^2/(1+\frac{1}{2}K^2) \sim 1/nN$, or rms equivalent divergence of [3]

$$\sigma_{r'} = \frac{1}{2\gamma}\sqrt{\frac{1+\frac{1}{2}K^2}{nN_{\text{p}}}} = \sqrt{\frac{\lambda_n}{2L}}, \qquad (4)$$

here $L = N_{\text{p}}\lambda_{\text{p}}$ is undulator length. Photons outside of the central cone are also outside of the undulator bandwidth (3) due to Doppler shift, as seen in (1). Only a small fraction of the total number of photons produced by an undulator is useful in experiments, which usually require a narrow bandwidth, since $\sigma_{r'}$ is much smaller than γ^{-1} (the natural angle of SR as determined by applying a Lorentz transformation to dipole radiation in the reference frame moving along with electron with velocity $c\bar{\beta}_z$) [4]. Therefore, by applying a "pin-hole" aperture corresponding to $\sigma_{r'}$, essentially white undulator radiation ($\Delta\lambda/\lambda \sim 1$) is selected to provide narrow peaks in the spectrum. This comes with a price of discarding most of undulator radiation, so that the fraction of photons in the central cone is roughly $\sim (\sigma_{r'}/\gamma)^2$ of the total number of photons produced in the undulator.

Formulae (1), (3) and (4) can be obtained by considering interference of wavefronts by *the same electron* at different points in the magnet [5]. In particular, the central cone divergence can be found as a variation of the angle at which interference becomes destructive for fixed wavelength. This is the same requirement as for a transverse coherent source in Fraunhofer approximation. Therefore, the radiation in the central cone from perfect electron beam is transversely coherent. This statement also can be demonstrated by means of a Young double-slit experiment. Interference pattern from the slits is destroyed when $bd/R \sim \lambda$, where *b* is source size, *d* is distance between the slits, *R* is distance from the source to the plane of the slits. The apparent source size (Fig. 1) of

undulator is simply $L\sigma_{r'}$, and with $d/R \sim \sigma_{r'}$ one finds that $\sigma_{r'} \sim \sqrt{\lambda/L}$, which is in qualitative agreement with (4).

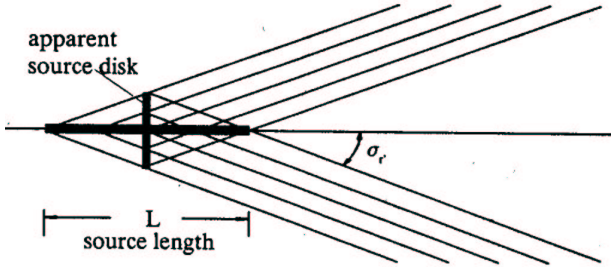

Fig. 1. Undulator apparent source size [from H. Wiedemann, Part. Acc. Phys, vol. 1]

The flux (photons/s) for the n^{th} harmonic in the central cone (i.e. useful photons) is given by [3]

$$\dot{N}_{\text{ph}}\Big|_n = \pi\alpha N_{\text{p}} \frac{\Delta\omega}{\omega_n}\frac{I}{e} g_n(K) \le \pi\alpha \frac{I}{e}\frac{g_n(K)}{n}, \qquad (5)$$

here α is fine structure constant, e is electron charge, and function $g_n(K) = nK^2[JJ]/(1+\frac{1}{2}K^2)$ with $[JJ]$ given by Bessel functions for the argument $x = \frac{nK^2}{4+2K^2}$: $[JJ] = [J_{(n-1)/2}(x) - J_{(n+1)/2}(x)]^2$. The function $g_n(K)$ is shown in Fig. 2. In practical units the maximum flux in the central cone is given by $\dot{N}_{\text{ph}}\Big|_n [ph/s] = 1.431\times10^{17} I[A] g_n(K)$.

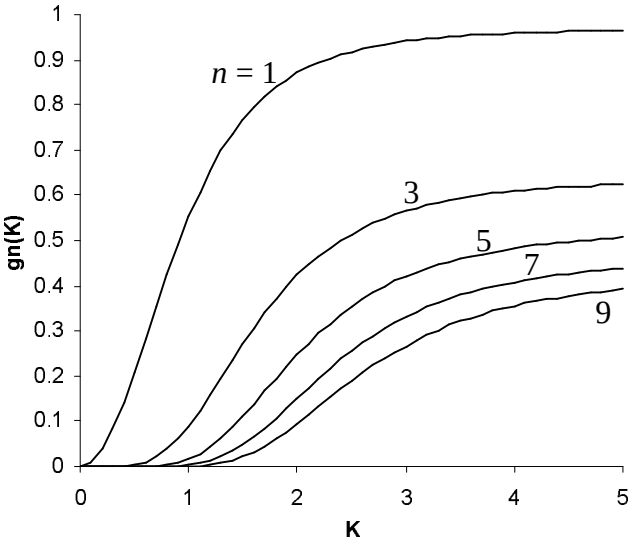

Fig. 2. Function $g_n(K) = nK^2[JJ]/(1+\frac{1}{2}K^2)$.

It is worth pointing out two things about the flux in the central cone. First, it is seen in (5) that the flux in the central cone does not depend on electron beam energy. This

indicates that an undulator operating at lower energies is as good as that operating at higher energies if *K* value in both cases is the same. However, besides the need to reduce the undulator period to deliver hard X-rays, *K* value also decreases with the period shortening since $K \sim \lambda_p \propto \gamma^{-2}$. As seen in Fig. 2, it is advantageous to have undulator strength parameter *K* to be at least 1 or so, and therefore, at some point reduction of the beam energy will compromise undulator performance. Second observation relates to the fact that the *maximum* flux in the central cone is independent from the number of poles N_p. This is in agreement with the fact that apparent source size increases as undulator becomes longer and the opening angle of the central cone decreases with its flux being independent from N_p. This is "the narrowing of the central cone", as it is sometimes referred to in the literature, with the maximum flux given by (5). For a moderate number of undulator poles ($N_p \sim 100$), the bandwidth of the central cone is only 1 %, while in many experiments the desired bandwidth is 10^{-4}. It means that the whole maximum flux in the central cone is rarely used, but only its fraction is selected with a monochromator. In this case (i.e. $N_p \le (n \cdot \text{bandwidth})^{-1}$), the number of photons which arrive at the sample does increase linearly with the number of poles. Finally, we observe from (5) that a high beam current *I* is important for photon production (or electron brightness, $I/\varepsilon_\perp^2$, for coherent photon production).

It is illustrative to calculate efficiency of an undulator, i.e. the ratio of power in the central flux for n^{th} harmonic to the total radiated power, P_{tot}:

$$\eta_{und} = \frac{\dot{N}_{ph}\big|_n n\hbar\omega_1}{P_{tot}} = \frac{3g_n(K)}{K^2(1+\frac{1}{2}K^2)}\frac{\Delta\omega}{\omega_n}n \le \frac{3g_n(K)}{K^2(1+\frac{1}{2}K^2)}\frac{1}{N_p}. \qquad (6)$$

For $K \to 0$, $\eta_{und,max} = 3/N_p$, but $P_{tot} \to 0$; and for $K \sim 1$ we have $\eta_{und,max} \sim 1/N_p$. Usually the bandwidth used in experiment, $(\Delta\omega/\omega)_{exp}$, is smaller than the undulator natural bandwidth (3), so undulator efficiency can be written simply as

$$\eta_{und} \sim (\Delta\omega/\omega)_{exp} \qquad (7)$$

Finite beam emittance and energy spread

The flux in the central cone (5) can be looked at as a pool of potentially useful photons. All these photons are transversely coherent when electron beam has no emittance. When electron beam has a finite emittance, only a (small) fraction from the pool is coherent, and even the smaller fraction reaches the sample after selection of a narrower bandwidth $(\Delta\omega/\omega)_{exp}$. The pool of useful flux for ERL for undulator with *arbitrary* number of poles is: average of 10^{16} *ph/s*, peak of $1.5 \cdot 10^{18}$ *ph/s* for 2 *ps* rms bunch duration or peak of $3 \cdot 10^{19}$ *ph/s* for 100 *fs* bunch duration. Transversely coherent flux F_{coh} is a fraction of the radiation in the central cone radiation, which is given by the ratio of 4D phase space area of photons from cold electrons to a convoluted with electrons 4D phase space area.

Assuming, somewhat simplistically, the optimal beta-function of electron beam matching the photon beam: $\varepsilon_{\rm ph} / \sigma_{r'}^2 = L / 2\pi$, we can write

$$F_{\rm coh} = \frac{\dot{N}_{\rm ph}}{(1+\varepsilon_\perp / \varepsilon_{\rm ph})^2}, \qquad (8)$$

with $\dot{N}_{\rm ph}$ given by (5), $\varepsilon_\perp$ being transverse electron emittance, which, in the case of round ERL beam, is on the order of 1 Å, and photon emittance (diffraction limit) given by $\varepsilon_{\rm ph} = \lambda / 4\pi$. In passing we notice that for a flat beam, as common to storage rings, with horizontal and vertical emittances $\varepsilon_{x,y}$, the coherent flux (or for that matter brilliance) is the same as for the round beam with emittance $\varepsilon_\perp = \sqrt{\varepsilon_x \varepsilon_y}$ when $\varepsilon_{x,y} >> \varepsilon_{\rm ph}$. Improvements in decoupling of the vertical and horizontal betatron motions in the storage rings result nowadays in very small vertical emittance, which starts to approach the diffraction limit $\varepsilon_y \sim \varepsilon_{\rm ph}$. In this case, however, it is more advantageous to have a round beam with $\varepsilon_\perp = \sqrt{\varepsilon_x \varepsilon_y}$ than a "pancake" beam because photon emittance is the same in both planes.

Coherent *average* flux for an ERL undulator then becomes (at 1 Å wavelength): average coherent flux – $5 \cdot 10^{13}$ *ph/s*; peak coherent flux – $8 \cdot 10^{16}$ *ph/s* for 2 *ps* bunches and $1.6 \cdot 10^{17}$ *ph/s* for 100 *fs* assuming no emittance degradation. Bandwidth selection to less than $1/N_{\rm p}$ further reduces this number.

Let us estimate photon power budget of ERL. From ERL II parameter list, we have about 200 *kW* total undulator radiation from 200 *m* net undulator length, i.e. 1 *kW* per 1 *m* of insertion device. This radiation is mostly white, so, when reducing the photon bandwidth to 10^{-3} or 10^{-4} we retain 1 or 0.1 *W* per 1 *m* of insertion device. This is useful radiation. If we desire to go one step further and work with coherent radiation, we will have 5 *mW* or 0.5 *mW* of coherent radiation per 1 *m* of insertion device for 10^{-3} or 10^{-4} bandwidth respectively. Peak power is 77 *pC*/(2 *ps* $\sqrt{2\pi}$) / 0.1 *A* = 150 times higher or 3000 times higher for 100 *fs* bunches. This radiation can be either redistributed among many users by utilizing shorter undulators, or all concentrated on a single experiment by using a longer undulator.

So far we have ignored beam energy spread. From (1) it can be seen that energy spread σ_γ / γ broadens the spectrum. Rms photon bandwidth due to the beam energy spread $\Delta\lambda / \lambda = 2\sigma_\gamma / \gamma$, or FWHM broadening is given by

$$\frac{\Delta\lambda}{\lambda} \approx 4.7 \frac{\sigma_\gamma}{\gamma} \qquad (9)$$

By comparing (9) with (3) we find that an undulator with the number of poles

$N_{\mathrm{p},\sigma_\gamma} \approx 0.2/n(\sigma_\gamma/\gamma)$ matches the broadening from electrons. It means that the bandwidth of photons in the central cone for an undulator with the number of poles bigger than $N_{\mathrm{p},\sigma_\gamma}$ remains the same, equal to (9). Energy spread from 2 ps rms bunch, after it traverses 1.3 GHz linac in phase with RF field, is about $2\cdot10^{-4}$, i.e. maximal $N_{\mathrm{p},\sigma_\gamma} \sim 1000$. If the bunch is run 10° off-crest with respect to the RF wave, the energy spread is $3\cdot10^{-3}$, i.e. $N_{\mathrm{p},\sigma_\gamma} \sim 70$. Beam energy spread does not effect transverse coherence to the first order (i.e. max flux in the central cone is still given by (5)), but it further reduces the number of photons in the narrow bandwidth for a fixed pin-hole aperture. The effect of electron beam emittance and energy spread can be further illustrated by evaluating the number of photons per quantum mode, or the number of photons in the coherence volume, which is degeneracy parameter, Δ_{coh} [6]. Degeneracy is simply $\Delta_{\mathrm{coh}} = F_{\mathrm{coh}} \cdot t_{\mathrm{coh}}$, with F_{coh} being the peak coherent flux introduced earlier (8), t_{coh} being longitudinal coherence time $t_{\mathrm{coh}} \sim (\lambda^2/\Delta\lambda)/c$. Degeneracy is invariant, i.e. determined by the source and cannot be improved with X-ray optics. We write the maximum achievable degeneracy as

$$\Delta_{\mathrm{coh}} \sim 2\cdot10^{-3} \frac{g_1(K)}{(1+\varepsilon_\perp/\varepsilon_{\mathrm{ph}})^2} \frac{\lambda_1}{\varepsilon_z} N_e, \qquad (10)$$

here $\varepsilon_z = \sigma_z\sigma_\gamma/\gamma$ is longitudinal emittance of electron beam, σ_z and N_e are rms bunch length and number of electrons in a single bunch respectively. For ERL, $\varepsilon_z \sim 10^{-7}$ *m*, $N_e \sim 5\cdot10^8$, so we find $\Delta_{\mathrm{coh}} \sim 5$. As seen from (10), the photon degeneracy is determined by electron density in 6D phase space. One might ask: what minimum longitudinal emittance might be achievable in ERL. It is hard to say definitively, but to the first order there is no uncorrelated emittance growth in the linac. After applying correction (or compressing bunch in several steps), final emittance theoretically can be as low as $(\gamma\varepsilon_z)_{\mathrm{inj}}/\gamma_{\mathrm{final}}$. In the injector, $\gamma\varepsilon_z = 6\cdot10^{-7}$ *m*, i.e. in principle one could think that $\varepsilon_z \sim 10^{-10}$ *m* is achievable at 5 GeV. However, there is uncorrelated energy spread due to quantum fluctuations $\sigma_\gamma/\gamma\big|_{\mathrm{rad}} \sim 10^{-5}$ at 5 *GeV*. Correlated emittance growth from RF waveform, which is proportional to σ_z^2, can be alleviated by compressing bunches in the linac in several stages. That, however, will make other effects more salient, such as coherent SR, wakes, power deposited in higher order modes, etc. This problem requires a more careful study. So, assuming that there is no additional bunch compression in the linac, and that the correlated energy spread from RF waveform is removed in the ring, we can have longitudinal emittance of $\varepsilon_z \sim \sigma_z \times \sigma_\gamma/\gamma\big|_{\mathrm{rad}} \sim 10^{-8}$ *m*, and maximum photon degeneracy $\Delta_{\mathrm{coh}} \sim 50$ respectively.

II. Self-amplified spontaneous emission (SASE)

It was shown in the previous section that undulator is generally quite inefficient as a source of coherent radiation. The coherent fraction of SR from an undulator is only

$(\Delta\lambda/\lambda)(\varepsilon_\perp/\varepsilon_{\rm ph})^2$ of the total emitted power, i.e. ~ 10^{-6} for ERL emittance and bandwidth of ~ 10^{-4}. SASE is a mechanism of radiation production that can be used to dramatically increase coherent flux if undulator is sufficiently long and electron density in 6D phase space is sufficiently high. Numerous references are available on the subject (e.g. see [7-15]). SASE radiation has very different characteristics as compared to spontaneous SR. SASE radiated power is comparable to the total spontaneous SR power emitted by the undulator at moderate beam energies of several *GeV*s (at higher energies SASE power is only a small fraction of the total radiated power, e.g. for LCLS it is 8 % of spontaneous SR). However, all SASE radiation is transversely coherent, similar to spontaneous SR in the central cone when $\varepsilon_\perp \sim \varepsilon_{\rm ph}$. Characteristics of longitudinal coherence of SASE, on the other hand, are similar to spontaneous SR in the central cone from the undulator of comparable length.

SASE FEL basic formulae

If a laser-like radiation with the wavelength according to (1) is present in an undulator, undulator magnetic field and light electromagnetic wave may act on the bunch to lead to a collective instability ("microbunching" on the scale of radiation wavelength) during the single pass through the insertion device, producing exponential growth of radiation [14]. In SASE, radiation is amplified from the initial noise, i.e. coherent fraction of SR discussed in the previous section.

A single most important SASE parameter is FEL efficiency, ρ, which is given by [9]

$$\rho = \left[\frac{K^2[JJ]r_e n_e \lambda_{\rm p}^2}{32\pi\gamma^3}\right]^{1/3} \qquad (11)$$

here r_e is electron classical radius, n_e is electron density: $n_e = N_e/[\sigma_x\sigma_y\sigma_z(2\pi)^{3/2}]$, and $[JJ]$ is same as defined before for the fundamental. Typically, ρ is between 10^{-3} to 10^{-4} for SASE X-FELs. This parameter describes SASE process, in particular:

1. SASE radiation power at saturation is given by $P_{\rm sat} \sim \rho \cdot P_{\rm beam}$, here $P_{\rm beam}$ is electron beam power $P_{\rm beam}[GW] = E[GeV]\cdot I[A]$.
2. Number of poles for undulator to reach saturation is $N_{\rm p,sat} \sim 1/\rho$, i.e. 10^3 to 10^4 poles.
3. Energy spread of initially monochromatic electron beam after saturation is on the order of ρ.

From the last point we conclude that SASE process does not preclude energy recovery as long as ρ << dump energy / full energy, i.e. ρ ~ 10^{-4} for present ERL II specs. By increasing the injection energy SASE can be operated with higher efficiency parameter ρ. Emittance degradation in the undulator is small and should not be a problem for energy recovery either [16]. Therefore, ERL based SASE FEL appears feasible at first glance, as also seen from the fact that both ERLs which existed so far have been used to drive FELs [17].

Power gain length of SASE is determined, according to 1D FEL theory [11], by

$$L_{G,1D} = \frac{\lambda_p}{4\pi\sqrt{3}\rho}. \qquad (12)$$

The gain length determines the rate of exponential growth of SASE power in the undulator. After about $20\times L_{G,1D}$ radiation power stops growing and saturation takes place. There are three requirements for efficient SASE process:

a) small transverse emittance of electron beam, i.e. electrons must match the transverse phase space of the radiation: $\varepsilon_\perp \le \varepsilon_{ph}$; (13a)

b) small energy spread: $\sigma_\gamma / \gamma < \rho$; (13b)

c) $L_G \le L_R$, here the Rayleigh range is given by $L_R = 4\pi\sigma_x^2/\lambda$, i.e. to avoid radiation escape due to diffraction. (13c)

When these conditions are satisfied, amplification is close to the optimum and analytical results of 1D FEL theory apply. If conditions (13) are not met, SASE effectiveness is quickly degraded in comparison with the 1D FEL theory.

An important comment about conditions (13) is the fact that these requirements apply to "slices" in the electron bunch. Electrons in the undulator lag behind radiation by λ in one undulator period, so that in SASE electrons interact with each other (via wiggling magnetic field and radiation) over the so-called cooperation length L_c, given by $L_c = \lambda\cdot(L_G/\lambda_p)$ typically much smaller than the bunch length. If slice characteristics of electron bunch meet the requirements of (13), SASE takes place. Slice length is about $2\pi L_c$, i.e. typically a fraction of 1 micron for X-FELs. As a result, SASE radiation temporal profile consists of $\sigma_z/(2\pi L_c)$ spikes, typically about 100 spikes for the bunch length of σ_z/c ~ 100 *fs*. Total energy distribution between the spikes is a Gamma function with $1/\sqrt{N_{spikes}}$ rms value. Even if there is no pulse-to-pulse fluctuations in the electron bunch parameters, SASE radiation has pulse-to-pulse intensity jitter of $1/\sqrt{100}$ ~ 10 %. Of course, radiation characteristics integrated over the whole bunch length will be determined by "projected" electron emittance and energy spread, rather than "slice" parameters, but the number of photons in 6D phase space (degeneracy) will be significantly higher when compared with spontaneous SR because of SASE enhancement.

Obtaining saturation power, gain length and saturation length for more realistic beam parameters than those of (13) generally requires numeric simulations. However, 1D SASE theory can be extended to a more general case [18]. The results of Ref. 18 have been used to optimize LCLS parameter space and are found in excellent agreement with computer codes simulations [7].

Here we use the results of Ref. 18. Actual power gain length, L_G, is longer than that

given by (12): $L_{G,1D}/L_G = 1/(1+\eta)$, here $\eta = \eta(\eta_d, \eta_{\varepsilon_\perp}, \eta_\gamma)$ is a universal scaling function, determined by fitting numerical solutions of coupled Maxwell-Vlasov equations describing FEL interactions, and

$$\eta_d = \frac{L_{G,1D}}{L_R}, \qquad \eta_{\varepsilon_\perp} = \frac{L_{G,1D}}{\beta}\frac{4\pi\varepsilon_\perp}{\lambda}, \qquad \eta_\gamma = 4\pi\frac{L_{G,1D}}{\lambda_p}\frac{\sigma_\gamma}{\gamma},$$

β here is beta-function. The scaling parameters $\eta_d, \eta_{\varepsilon_\perp}$, and η_γ measure the deviation of the beam from the ideal 1D case $\eta(0,0,0) = 0$. Specifically, η_d is for gain reduction due to diffraction, a spatial 3D effect, $\eta_{\varepsilon_\perp}$ and η_γ are for gain reduction due to electron's longitudinal velocity spread caused by emittance and by energy spread respectively (cf. (13)). $\eta = \eta(\eta_d, \eta_{\varepsilon_\perp}, \eta_\gamma)$ is given in [18]. Saturation length is determined from $L_{sat} = L_G \ln(P_{sat}/\alpha_c P_{noise})$, with saturation power $P_{sat} \approx 1.6\rho(L_{G,1D}/L_G)^2 P_{beam}$, effective input noise power $P_{noise} \approx \rho^2 cE/\lambda$ for the average beam energy *E*, the coupling coefficient of P_{noise} into the dominant exponentially growing mode $\alpha_c = 1/9$.

SASE performance for different bunch parameters

Three sets of beam parameters were studied as applicants to drive SASE radiation: 1) nearly nominal ERL parameters for 77 *pC* bunch without bunch compression; 2) 77 *pC* per bunch compressed to 100 *fs*; 3) "dream" parameter list similar to LCLS bunch specs, although somewhat relaxed. In all three cases slice emittance was assumed to be 1 Å, which is currently being demonstrated with the injector simulations for ERL prototype for bunches of 77 *pC* (i.e. < 1 μm normalized emittance at $\gamma = 10^4$, see [19]). Energy spread listed in Cases 2 and 3 refers to the maximum allowable energy spread that causes increase of saturation length of 10 % if compared to monoenergetic beam with otherwise the same parameters. The total energy spread is estimated as slice energy spread times the number of spikes, which, in turn, is found as $N_{spikes} \sim \sigma_z / 2\pi L_c$ (i.e. the correlated component of the energy spread dominates over the uncorrelated part). Furthermore, in all three cases minimum allowable undulator gap was assumed to be 6 mm, and average beta-function in undulator is 7 m (same as in LCLS proposal [7]). Maximum magnetic field in undulator is given by (2).

Case 1

Beam energy	5 GeV
Charge per bunch	77 pC
Normalized slice emittance (rms)	1 mm-mrad
Bunch length (rms)	0.6 mm
Peak current	15 A
Average beta-function	7 m
Slice fractional energy spread	$<< \rho$

In this case peak current is small and, as expected, SASE process is rather inefficient, requiring unrealistically long undulator. See Fig. 3. Thus, case 1 is not interesting for SASE.

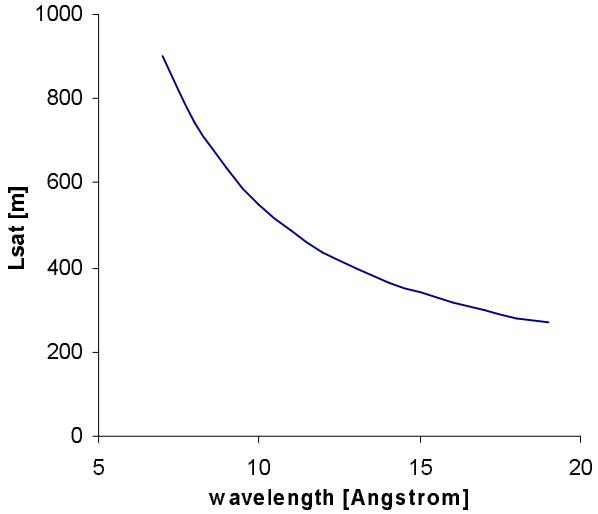

Fig. 3. Case 1: net undulator length required to reach saturation

Case 2

Beam energy	5 *GeV*
Charge per bunch	77 *pC*
Normalized slice emittance (rms)	1 *mm-mrad*
Bunch length (rms)	0.03 *mm*
Peak current	0.3 *kA*
Average beta-function	7 *m*
Slice fractional energy spread	1.8×10^{-4}
Total fractional energy spread	1.3×10^{-3}

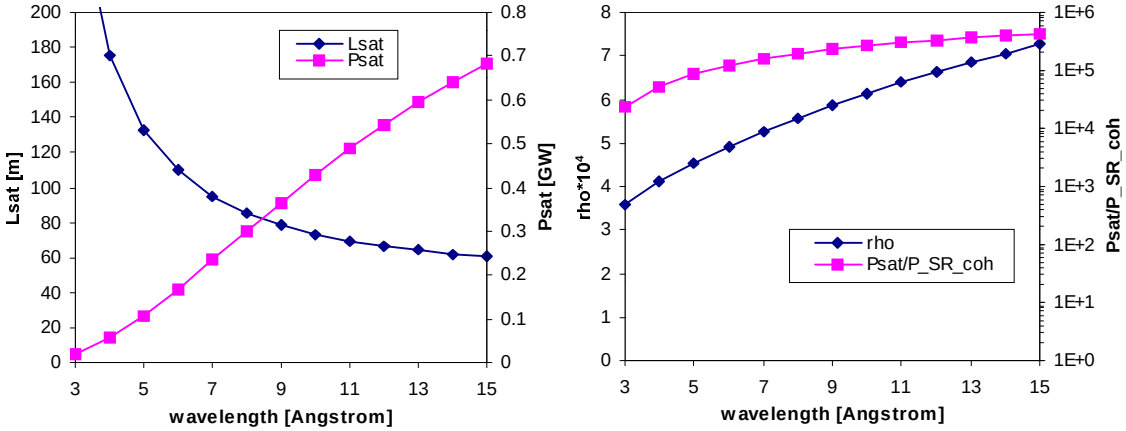

Fig. 4. Case 2: saturation length and peak power (left); ρ and ratio of SASE coherent power to spontaneous SR coherent power as given by (8) (right).

As seen in Fig. 4, saturation length is about 95 *m* for 7 Å radiation wavelength. SASE

enhances coherent flux by 5 orders of magnitude as compared with usual SR radiation. *K* value at 7 Å is about 2.8, i.e. the 3rd harmonic will also be generated. It may be enhanced by SASE as well with radiation power level of about 10^{-2} of the fundamental [7]. Thus, one could expect ~ *MW* coherent power at 2.3 Å wavelength, i.e. still about 3 orders of magnitude higher than the coherent fraction of spontaneous SR power.

Case 3

Beam energy	5 *GeV*
Charge per bunch	770 *pC*
Normalized slice emittance (rms)	1 *mm-mrad*
Bunch length (rms)	0.03 *mm*
Peak current	3 *kA*
Average beta-function	7 *m*
Slice fractional energy spread	2.9×10^{-4}
Total fractional energy spread	9.0×10^{-3}

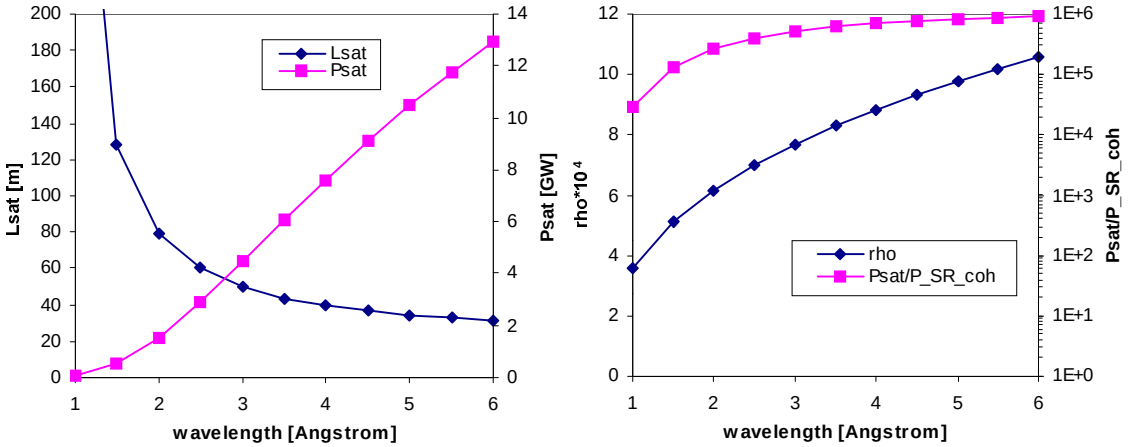

Fig. 4. Case 3: saturation length and peak power (left); ρ and ratio of SASE coherent power to spontaneous SR coherent power as given by (8) (right).

In this case, the saturation length at 2 Å is about 80 *m*, peak SASE power is on the order of *GW* level, which is 5 orders of magnitude higher than the coherent power from spontaneous SR radiation. *K* value in this case is 1.4, i.e. harmonic content will be weaker. In both cases 2 and 3, FEL efficiency parameter ~ $5\cdot10^{-4}$ and the undulator period length is 2.7 and 2.0 cm respectively.

Conclusions

ERL II will be a modest source of coherent radiation when using spontaneous radiation from undulators in comparison to SASE X-FELs sources. Its performance is to be compared with the best of the 3rd generation synchrotron light sources. Each 77 *pC* bunch will produce about 200 transversely coherent photons at 1 Å wavelength in the bandwidth of 10^{-4} per 1 meter of insertion device if the beam relative energy spread can be kept on the level of 10^{-4}. For SASE, on the other hand, each bunch could produce 10^9 coherent photons at 7 Å within 10^{-4} bandwidth for beam with parameters of Case 2 from

a hundred-meter-long undulator or ~ 10^7 photons per 1 meter of undulator (for SASE, however, undulator *has* to be long to obtain necessary gain and saturation unlike for spontaneous SR). Possibility of the 3rd harmonic generation would extend Case 2 SASE to about 2.3 Å. For beam parameters close to LCLS proposal (Case 3), each bunch with the charge 10 times higher than 77 *pC* would produce ~ 10^7 coherent photons within 10^{-4} bandwidth per 1 m of undulator, but now at the wavelength of 2 Å. Furthermore, the average flux in the central cone (i.e. useful flux) is about 4-5 orders of magnitude higher in the case of SASE as opposed to spontaneous SR for the same average beam current. That is, if SASE can be secured, a beam of 10 μA average current would produce the same flux as ERL II 100 mA beam without SASE. Obvious disadvantages of SASE are seen in the poor pulse-to-pulse intensity stability, which is likely to be ten percent or more [7], a limited number of X-ray beam lines, difficulty to secure the necessary high electron density in 6D phase space, and very long undulator required to reach saturation. Besides, SASE is likely to be out of reach for harder X-rays (0.1 Å). In this spectral range, however, there should be rich high harmonic content from usual undulator radiation. SASE's advantages, on the other hand, are also obvious.

Acknowledgements
Interactions with the following people on the subject of undulator radiation and coherence is gratefully acknowledged: Don Bilderback, Ken Finkelstein, Alexander Kazimirov, Qun Shen, Richard Talman.

References

1. K. Halbach, J. de Physique, C1, suppl. no 2, Tome 44 (1983)
2. D.F. Alferov, et al., Pis' ma v Zhurnal Tekhnicheskoi Fiziki, 12 (1976) 487
3. K.J. Kim, AIP Conf. Proc., 189, issue 1, pp. 565-632, 1989
4. This statement is in the agreement with Richard Talman's argument that there is no "narrowing of the cone" for SR from undulator; see R. Talman, LNS tech. note CBN 00-10. This is also in no conflict with the lore of the field as it is seen further.
5. E.g., see CERN Accelerator School Proc., CERN 98-04, p.129
6. B. Lengeler, Naturwissenschaften, 88 (2001) 249
7. LCLS CDR, http://www-ssrl.slac.stanford.edu/LCLS/CDR/
8. C. Pellegrini, NIMA 272 (1988) 364
9. K.J. Kim, et al., NIMA 239 (1985) 54
10. J. Murphy and C. Pellegrini, NIMA 237 (1985) 159
11. R. Bonifacio, et al., Opt. Com., 50 (1984) 373
12. R. Bonifacio, et al., Phys. Rev. Lett., 73 (1994) 70
13. W.B. Colson and J. Blau, NIMA 272 (1988) 386
14. W.B. Colson and A.M. Sessler, Ann. Rev. Nuc. Sci., 1984 (35) 25
15. W.B. Colson, NIMA 393 (1997) 82
16. The main mechanism of emittance degradation in SASE would be quantum fluctuations. The effect of quantum fluctuations on transverse electron motion remains low because of small dispersion in undulator, e.g. see ERL Study.
17. That is Stanford SCA/FEL and JLAB IR FEL.
18. Ming Xie, IEEE PAC Proc., 0-7803-3053-6 (1996) 183
19. e.g. see I.V. Bazarov, ERL site visit presentation, March 2002